

DISCOVERY OF SUPERSTRONG, FADING, IRON LINE EMISSION AND DOUBLE-PEAKED BALMER LINES OF THE GALAXY SDSS J095209.56+214313.3: THE LIGHT ECHO OF A HUGE FLARE

S. KOMOSSA,¹ H. ZHOU,^{1,2} T. WANG,² M. AJELLO,¹ J. GE,³ J. GREINER,¹ H. LU,² M. SALVATO,⁴ R. SAXTON,⁵
H. SHAN,⁶ D. XU,⁷ AND W. YUAN⁶

Received 2008 February 12; accepted 2008 March 17; published 2008 March 27

ABSTRACT

We report the discovery of superstrong, fading, high-ionization iron line emission in the galaxy SDSS J095209.56+214313.3 (SDSS J0952+2143 hereafter), which must have been caused by an X-ray outburst of large amplitude. SDSS J0952+2143 is unique in its strong multiwavelength variability; such a broadband emission-line and continuum response has not been observed before. The strong iron line emission is accompanied by unusual Balmer line emission with a broad base, narrow core, and double-peaked narrow horns, and strong He II emission. These lines, while strong in the SDSS spectrum taken in 2005, have faded away significantly in new spectra taken in 2007 December. Comparison of SDSS, 2MASS, *GALEX*, and follow-up GROND photometry reveals variability in the NUV, optical, and NIR band. Taken together, these unusual observations can be explained by a giant outburst in the EUV–X-ray band, detected even in the optical and NIR. The intense and variable iron, helium, and Balmer lines represent the “light echo” of the flare, as it traveled through circumnuclear material. The outburst may have been caused by the tidal disruption of a star by a supermassive black hole. Spectroscopic surveys such as SDSS are well suited to detect emission-line light echoes of such rare flare events. Reverberation-mapping of these light echoes can then be used as a new and efficient probe of the physical conditions in the circumnuclear material in nonactive or active galaxies.

Subject headings: galaxies: active — galaxies: evolution —
galaxies: individual (SDSS J095209.56+214313.3) — quasars: emission lines

1. INTRODUCTION

The continuum emission of many active galactic nuclei (AGNs) is variable by a factor of a few. The broad-line region (BLR) emission-line response to changes in the ionizing continuum provides us with important information on the size and physical properties of the emission-line clouds (see Peterson 2007 for a review). A few exceptional cases of nonrepetitive, i.e., transient, extreme broad-line variability have been reported, including the temporal appearance of an unusually broad He II line in NGC 5548 (Peterson & Ferland 1986), and of double-peaked Balmer lines in NGC 1097 (Storchi-Bergmann et al. 1993) and a few other LINERs, interpreted as a response to transient accretion events.

Detection of strong continuum and emission-line variability is of great interest, since it places tight constraints on accretion physics and physical conditions in the gas clouds surrounding the supermassive black hole (SMBH). High-amplitude variability of emission lines other than the classical broad lines is rare in AGNs. The one notable exception is the Seyfert galaxy IC 3599. X-ray bright during the *ROSAT* all-sky survey, a near-simultaneous optical spectrum showed strong high-ionization lines (Brandt et al. 1995) which were significantly fainter in a new optical spectrum taken 8 months later (Grupe et al. 1995). The X-ray flux and the high-ionization emission lines continued

to fade in subsequent years, and in low-state, the galaxy can be classified as a Seyfert 1.9 or 2. The X-ray flare of this active galaxy was interpreted in terms of a temporarily enhanced accretion rate (Brandt et al. 1995; Grupe et al. 1995; Komossa & Bade 1999).

The highest amplitudes of X-ray variability, up to factors of ~ 6000 , have been almost exclusively detected in nonactive galaxies, and these represent the best observational evidence to date for the process of tidal disruption of stars by SMBHs (e.g., Komossa & Bade 1999; Halpern et al. 2004; Komossa et al. 2004).

Here we report the discovery of very unusual and variable emission lines of the galaxy SDSS J0952+2143 at redshift $z = 0.079$, found in a systematic search for emission-line AGNs in SDSS DR6 (Sloan Digital Sky Survey Data Release 6; Adelman-McCarthy et al. 2008). The optical spectrum of SDSS J0952+2143 (Fig. 1) looked very similar, but more extreme, than that of IC 3599 in high state, which is why we suspected a similar mechanism at work and initiated the follow-up observations reported in this Letter. SDSS J0952+2143 turns out to be unique in its broad multiwavelength continuum and emission-line response to a high-energy outburst. We use a cosmology with $H_0 = 70 \text{ km s}^{-1} \text{ Mpc}^{-1}$, $\Omega_M = 0.3$, and $\Omega_\Lambda = 0.7$ throughout this Letter.

2. MULTIWAVELENGTH OBSERVATIONS AND RESULTS

2.1. SDSS Photometry in 2004

SDSS J0952+2143 was brightest during SDSS photometry performed on 2004 December 20. At that time it showed a flat spectral energy distribution (SED) with an increase toward the NIR, which was inconsistent with the extrapolation of 2MASS data taken in 1998 January (Fig. 2). The SDSS photometric data can be well described by a constant underlying galaxy SED and a power-law component consistent in shape with that

¹ Max-Planck-Institut für extraterrestrische Physik, Postfach 1312, 85741 Garching, Germany; skomossa@mpe.mpg.de.

² Center for Astrophysics, University of Science and Technology of China, Hefei, Anhui 230026, China.

³ Department of Astronomy, University of Florida, Gainesville, FL 32611.

⁴ California Institute of Technology, 105-24 Robinson, 1200 East California Boulevard, Pasadena, CA 91125.

⁵ ESA/ESAC, Apartado 78, 28691 Villanueva de la Canada, Madrid, Spain.

⁶ National Astronomical Observatories/Yunnan Observatory, Chinese Academy of Science, P.O. Box 110, Kunming, China.

⁷ National Astronomical Observatories, Chinese Academy of Science, A20 Datun Road, Chaoyang District, Beijing 100012, China.

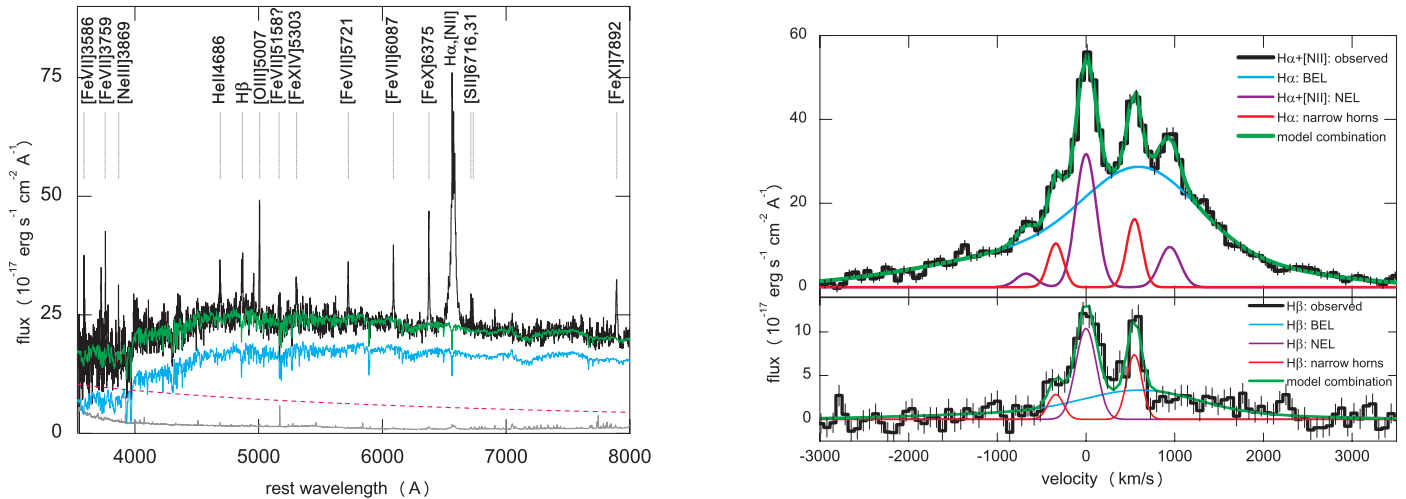


FIG. 1.—*Left*: SDSS spectrum of SDSS J0952+2143 (black), and continuum decomposition into stellar (blue) and power-law components (red). *Right*: Profiles of H α and H β , and decomposition into broad base (BEL), narrow core (NEL), and two narrow horns.

during the SDSS spectroscopy 1 year later, but of greater strength. The increase toward the NIR can be described by an extra blackbody component with a temperature of 2400 K.

2.2. SDSS Spectroscopy in 2005

Spectroscopy of SDSS J0952+2143 was performed on 2005 December 30. It was fainter than during the photometry. The continuum SED can be decomposed into a host-galaxy contribution and a power law of index $\alpha = -1.0$, where $f_{\lambda} \propto \lambda^{\alpha}$. The bulk of the variability between 2004 December and 2005 December can be attributed to a variable power-law component which was fainter by a factor of 2 in 2005.

During the 2005 spectroscopy, SDSS J0952+2143 displayed a rich and unusual emission-line spectrum. A variety of high-ionization iron coronal lines from [Fe VII] and up to [Fe XIV] can be identified, several with unprecedented strengths relative to [O III] $\lambda 5007$, and several as strong as [O III] (Fig. 1 and Table 1). Transitions include [Fe VII] $\lambda\lambda 3586, 3759$, rarely identified in AGNs. Iron lines consist of a broad (FWHM $\approx 700\text{--}800 \text{ km s}^{-1}$) and a narrow (FWHM $\approx 100\text{--}150 \text{ km s}^{-1}$) component. Strong He II $\lambda 4686$ emission is present with a width similar to the broad component of the iron lines [FWHM(He II) = 810 km s^{-1}]. The Balmer line profile shows multiple components. A multi-Gaussian decomposition reveals a broad base [FWHM(H α_b) = 1930 km s^{-1} , where the index b denotes the broad component of the profile], a narrow core (FWHM fixed to that of [S II] $\lambda\lambda 6716, 6731$; 200 km s^{-1}), and two remarkable unresolved narrow horns (Fig. 1). The broad base is redshifted by 570 km s^{-1} and has a luminosity of $L_{\text{H}\alpha_b} = 3 \times 10^{41} \text{ ergs s}^{-1}$. The two narrow horns are also prominent in H β , while its broad component is barely detected, implying a ratio $\text{H}\alpha_b/\text{H}\beta_b = 9.5$.

Using stellar absorption lines detected in the spectrum, we have determined the stellar velocity dispersion, $\sigma_{*} = 95 \text{ km s}^{-1}$. This implies a black hole mass of $M_{\text{BH}} = 7 \times 10^6 M_{\odot}$ (Ferrarese & Ford 2005).

2.3. GALEX UV Photometry in 2006

The GALEX (Martin et al. 2005) UV photometric data points, of 2006 March 2, are above the expected host-galaxy contribution, and are consistent with the extrapolated power-law com-

ponent measured during SDSS spectroscopy ~ 2 months earlier (Fig. 2).

All these results locate the maximum of the outburst after the 2MASS observation in 1998, and possibly close to the 2004 SDSS photometry high state.

2.4. Optical and X-Ray Follow-ups in 2007 and 2008

In order to search for line variability, we have taken new optical spectra on 2007 December 4 and 5 with the OMR spectrograph equipped with a 200 \AA mm^{-1} grating at the Xinglong 2.16 m telescope. In these new optical spectra most of the iron lines, the He II line, and the broad H α line are significantly fainter *relative to* [O III] (Fig. 2). Broad H α , He II, and [Fe XIV] have faded by a factor of ~ 2 . [Fe X] is no longer detected. Despite the lower S/N of the Xinglong spectrum and the coincidence of telluric atmospheric absorption with the redshifted [Fe X], this still implies line variability by a least a factor of 2.

New photometry was performed with GROND, a multi-channel imager (Greiner et al. 2008) attached to the 2.2 m telescope at La Silla in the SDSS filters $g, r, i,$ and z on 2008 January 1, at a seeing of $1''$. These data confirm the decline in the optical and NIR band. The core of SDSS J0952+2143 (the central $1.4'' \times 1.4''$) was a factor 2 weaker than during the 2004 SDSS photometry.

We have initiated a *Chandra* DDT X-ray observation of 10 ks duration which was carried out on 2008 February 5. SDSS J0952+2143 was detected with an ACIS-S count rate of $0.0007 \text{ counts s}^{-1}$, corresponding to a 2–10 keV X-ray luminosity of $4 \times 10^{40} \text{ ergs s}^{-1}$ (S. Komossa et al., in preparation).

3. DISCUSSION

We have detected the emission-line light echo and the low-energy (NUV, optical, NIR) SED tail of a high-energy (EUV, X-ray) outburst of the galaxy SDSS J0952+2143. The EUV–X-ray part of the flare was not observed directly, but the presence of a strong ionizing continuum at high state is implied by the strong H α and He II lines and by the large iron-line fluxes relative to [O III]. Further, the ionization potentials of He II and of the iron lines (up to 358 eV; Fe XIV) imply that the ionizing continuum extended into the soft X-ray regime.

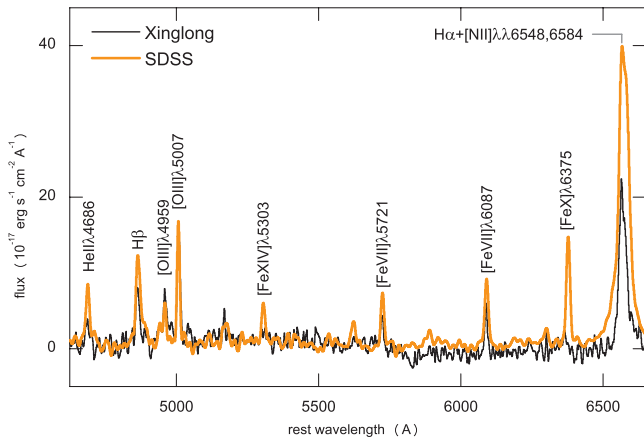


FIG. 2.—*Left*: Comparison of the new Xinglong spectrum of 2007 December (*black*) with the previous SDSS spectrum (*orange*; the resolution was degraded to match that of Xinglong). Both spectra have been continuum-subtracted, and scaled assuming constant [O III] flux. *Right*: UV–optical–NIR SED; data points and model fits as marked in the plot, taken at different epochs.

While X-ray variability is common in AGNs, amplitudes exceeding a factor of ~ 30 – 50 are rare (e.g., Komossa 2002) and they almost never come with a reported measurable emission-line response. Outbursts of high amplitude are of special interest, because they provide tight constraints on accretion physics under extreme conditions. Furthermore, as the flare travels through the circumnuclear material, its emission-line light echo puts us in the rare situation to be able to perform “reverberation mapping” not only of the BLR, but potentially also of the accretion disk region, the coronal-line region (CLR), the molecular torus, and the narrow-line region (NLR) of active galaxies (Ulmer 1999; Komossa & Bade 1999), and it allows us to detect which of these regions are also present in nonactive galaxies (Komossa 2002).

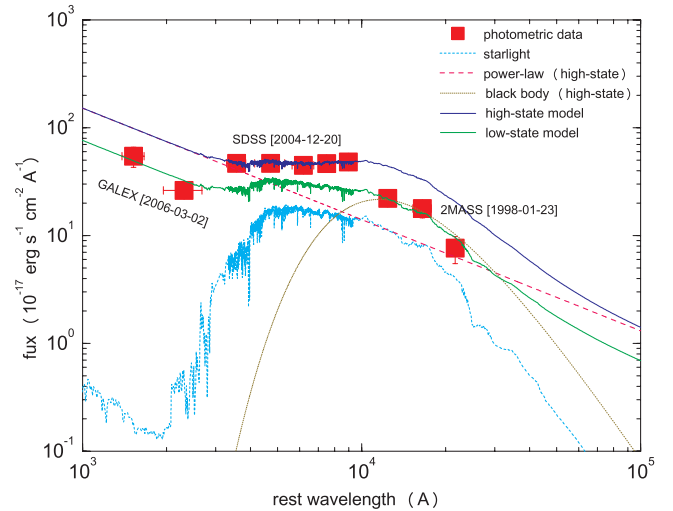
3.1. Amplitude of Variability, and Galaxy Classification

Since X-ray monitoring simultaneous with and after the SDSS observations does not exist, we can only indirectly estimate the amplitude of variability of the outburst. The fluxes of the iron lines, relative to [O III], observed in 2005 (1 year after the highest observed state in 2004), are much higher than

Line	Ratio
[Fe VII] $\lambda 3759$	0.7
He II $\lambda 4686$	0.7
$H\beta_{\text{total}}$	1.3 ^a
$H\beta_n$	0.4
[O III]	1.0
[Fe XIV] $\lambda 5303$	0.4
[Fe VII] $\lambda 6087$	0.7
[Fe X] $\lambda 6375$	1.3
H α	10.0 ^a
[S II] $\lambda 6725^b$	0.5
[Fe XI] $\lambda 7892$	1.0

^a Including the broad and narrow component, but not the two extra horns.

^b Sum of [S II] $\lambda 6716$ and [S II] $\lambda 6731$.



those in any other AGN in SDSS DR6. The observed (2005; post-high-state) ratio [Fe X]/[O III] is a factor of 60 (20) higher than the Seyfert 2 (Seyfert 1) average of Nagao et al. (2000, their Table 6), implying a high amplitude of variability.

It is possible that all emission lines were excited by the flare.⁸ Alternatively, SDSS J0952+2143 may show permanent low-level activity traced by low-ionization lines. The ratio [O III]/ $H\beta_n = 2.5$ puts the galaxy at the border between AGN and LINER.

3.2. NIR Variability

While the variable optical continuum likely is the tail of the high-energy continuum, the variable NIR continuum during the 2004 SDSS photometry high state is best fit by an independent blackbody component of $T \approx 2400$ K, perhaps a signal of dust reprocessing before destruction. The measured temperature slightly exceeds the sublimation temperature T_s of standard silicates and graphite (e.g., Granato & Danese 1994), but non-standard grain sizes and decomposition may raise the limit on T_s .

3.3. Iron Line Diagnostics

For the first time, transitions of [Fe VII] $\lambda\lambda 3586, 3759$ as strong as [O III] have been identified in a galaxy spectrum. Several [Fe VII] line ratios can be used to estimate gas temperature and gas density. The observed high-state ratio of [Fe VII] $\lambda 5158$ /[Fe VII] $\lambda 6087 \approx 0.2$ implies a density of $\log n_e = 6$ – 7 . The ratio [Fe VII] $\lambda 3759$ /[Fe VII] $\lambda 6087 = 1$ implies a temperature of at least $T \geq 20,000$ K, and up to $T = 50,000$ K if $\log n_e \leq 6$ (Keenan & Norrington 1987). The high density and temperature inferred and the variability of the iron lines on the timescale of years implies an emission region close to the active nucleus. Possible sites of origin of the observed lines are the inner wall of the dusty torus, and/or the tidal debris of

⁸ Given light-travel time delays, the bulk of any permanent low-density gas at NLR-typical distances will only be reached after a long time. However, the fraction of this gas that is close to our line of sight will already be illuminated by the flare. This mechanism would cause temporary AGN-like line emission even in intrinsically nonactive galaxies.

a disrupted star flung out from the system and interacting with its environment (Khoklov & Melia 1996). Monitoring of the fading lines will provide a key diagnostic of the physical conditions in the line-emitting region; if this region corresponds to the dusty torus, we can do “torus reverberation mapping” this way.

3.4. Double-peaked Balmer Line Emission

The H α and H β lines show a complex profile which can be decomposed into at least four components: a broad component with a width of 1930 km s⁻¹ redshifted by an extra 570 km s⁻¹, a narrow component at the same redshift as other narrow forbidden lines, and two narrow horns, the more conspicuous one redshifted by 540 km s⁻¹. Double-peaked Balmer lines have been detected in a number of AGNs (see Eracleous et al. 2006 for a review). However, generally, it is the *broad* component of the Balmer lines which is double peaked. The strong narrow horn has no counterpart in any other emission line; it is only detected in H α and H β . One possible explanation is that it arises in a region of very high density (such as the stellar postdisruption debris, or an accretion disk; see § 3.5) where forbidden lines are suppressed. The summed redshifted broad and narrow component of the H α profile resembles to some extent, but not in detail, relativistic Fe K α line profiles seen in some AGN X-ray spectra (review by Miller 2007). The broad Balmer decrement, H α /H β = 9.5, likely implies a significant contribution from collisional excitation indicative of high density, or else is affected by optical depth effects.

3.5. Outburst Mechanism

The highest amplitudes of variability detected to date, up to a factor of ~6000, have essentially all been observed from nonactive galaxies, and have been interpreted in terms of tidal disruptions of stars by supermassive black holes (Komossa & Bade 1999; Halpern et al. 2004; Komossa et al. 2004 and references therein). Stars approaching a SMBH will be tidally disrupted once the tidal forces of the SMBH exceed the star’s self-gravity, and part of the stellar debris will be accreted,

producing a luminous flare of radiation which lasts on the timescale of months to years (e.g., Carter & Luminet 1982; Rees 1988; see Komossa 2002 for a much longer list of references on theoretical aspects of tidal disruption).

The outburst mechanism of SDSS J0952+2143 is either related to processes in the accretion disk such as an instability (only possible if SDSS J0952+2143 is permanently active), or is else related to the tidal disruption of a star by the SMBH at its center (possible in both cases, active or nonactive galaxy); see Komossa & Bade (1999) for a discussion of relevant time-scales of both mechanisms. At present, we cannot tell whether SDSS J0952+2143 harbors a permanent low-luminosity AGN, traced by [O II] and [O III], or whether these lines were also excited by the flare and represent low-density ISM/NLR emission close to our line of sight.

In the context of tidal disruption, the unusual profile and double-peakedness of the Balmer lines can be understood as emission from the accretion disk formed from the stellar debris after disruption. While Balmer line emission from different streams of the disrupted star looks complex during the first several months after disruption (Bogdanovic et al. 2004), it would appear more like a normal disk line thereafter.

While automated procedures are currently being set up to identify new flares rapidly in the course of current X-ray surveys (Yuan et al. 2006; Esquej et al. 2007), spectroscopic surveys such as SDSS-II will allow us to perform independent flare searches by the detection of variable emission-line signatures. SDSS J0952+2143 is exceptional among the few known flaring galaxies in its strong multiwavelength variability, encompassing the NIR, optical, and NUV continuum SED, allowed and forbidden optical and NIR emission lines, and the EUV and X-ray SED. Such a broadband line and continuum response has not been detected before. Multiwavelength monitoring of objects such as SDSS J0952+2143 will enable us to follow the fading of the emission lines, providing a unique light echo mapping of the circumnuclear material, potentially including the accretion disk, BLR, torus, and ISM, and flung-out postdisruption stellar material if the cause of the flare was stellar tidal disruption.

REFERENCES

- Adelman-McCarthy, J. K., et al. 2008, ApJS, in press
 Bogdanovic, T., et al. 2004, ApJ, 610, 707
 Brandt, W. N., Pounds, K., & Fink, H. H. 1995, MNRAS, 273, L47
 Carter, B., & Luminet, J.-P. 1982, Nature, 296, 211
 Eracleous, M., et al. 2006, in ASP Conf. Ser. 360, AGN Variability from X-Rays to Radio Waves, ed. C. M. Gaskell et al. (San Francisco: ASP), 227
 Esquej, P., et al. 2007, A&A, 462, L49
 Ferrarese, L., & Ford, H. 2005, Space Sci. Rev., 116, 523
 Granato, G. L., & Danese, L. 1994, MNRAS, 268, 235
 Greiner, J., et al. 2008, PASP, in press
 Grupe, D., et al. 1995, A&A, 299, L5
 Halpern, J., et al. 2004, ApJ, 604, 572
 Keenan, F. P., & Norrington, P. H. 1987, A&A, 181, 370
 Khoklov, A., & Melia, F. 1996, ApJ, 457, L61
 Komossa, S. 2002, Rev. Mod. Astron., 15, 27
 Komossa, S., & Bade, N. 1999, A&A, 343, 775
 Komossa, S., et al. 2004, ApJ, 603, L17
 Martin, D. C., et al. 2005, ApJ, 619, L1
 Miller, J. M. 2007, ARA&A, 45, 441
 Nagao, T., et al. 2000, AJ, 119, 2605
 Peterson, B. M. 2007, in ASP Conf. Ser. 373, The Central Engine of Active Galactic Nuclei, ed. L. C. Ho & J.-M. Wang (San Francisco: ASP), 3
 Peterson, B. M., & Ferland, G. 1986, Nature, 324, 345
 Rees, M. J. 1988, Nature, 333, 523
 Storchi-Bergmann, T., et al. 1993, ApJ, 410, L11
 Ulmer, A. 1999, ApJ, 514, 180
 Yuan, W., et al. 2006, Adv. Space Res., 38, 1421